



# The mitochondria-targeted antioxidant MitoQ attenuated PM<sub>2.5</sub>-induced vascular fibrosis via regulating mitophagy

Ruihong Ning<sup>a,b</sup>, Yang Li<sup>a,b</sup>, Zhou Du<sup>a,b</sup>, Tianyu Li<sup>a,b</sup>, Qinglin Sun<sup>a,b</sup>, Lisen Lin<sup>a,b</sup>, Qing Xu<sup>c</sup>, Junchao Duan<sup>a,b,\*\*</sup>, Zhiwei Sun<sup>a,b,\*</sup>

<sup>a</sup> Department of Toxicology and Sanitary Chemistry, School of Public Health, Capital Medical University, Beijing, 100069, PR China

<sup>b</sup> Beijing Key Laboratory of Environmental Toxicology, Capital Medical University, Beijing, 100069, PR China

<sup>c</sup> Core Facilities Center, Capital Medical University, Beijing, 100069, People's Republic of China

## ARTICLE INFO

### Keywords:

Short-term PM<sub>2.5</sub> exposure  
Vascular fibrosis  
MitoQ  
Mitochondrial dysfunction  
Mitophagy

## ABSTRACT

Short-term PM<sub>2.5</sub> exposure is related to vascular remodeling and stiffness. Mitochondria-targeted antioxidant MitoQ is reported to improve the occurrence and development of mitochondrial redox-related diseases. At present, there is limited data on whether MitoQ can alleviate the vascular damage caused by PM<sub>2.5</sub>. Therefore, the current study was aimed to evaluate the protective role of MitoQ on aortic fibrosis induced by PM<sub>2.5</sub> exposure. Vascular Doppler ultrasound manifested PM<sub>2.5</sub> damaged both vascular function and structure in C57BL/6J mice. Histopathological analysis found that PM<sub>2.5</sub> induced aortic fibrosis and disordered elastic fibers, accompanied by collagen I/III deposition and synthetic phenotype remodeling of vascular smooth muscle cells; while these alterations were partially alleviated following MitoQ treatment. We further demonstrated that mitochondrial dysfunction, including mitochondrial reactive oxygen species (ROS) overproduction and activated superoxide dismutase 2 (SOD2) expression, decreased mitochondrial membrane potential (MMP), oxygen consumption rate (OCR), ATP and increased intracellular Ca<sup>2+</sup>, as well as mitochondrial fragmentation caused by increased Drp1 expression and decreased Mfn2 expression, occurred in PM<sub>2.5</sub>-exposed aorta or human aortic vascular smooth muscle cells (HAVSMCs), which were reversed by MitoQ. Moreover, the enhanced expressions of LC3II/I, p62, PINK1 and Parkin regulated mitophagy in PM<sub>2.5</sub>-exposed aorta and HAVSMCs were weakened by MitoQ. Transfection with PINK1 siRNA in PM<sub>2.5</sub>-exposed HAVSMCs further improved the effects of MitoQ on HAVSMCs synthetic phenotype remodeling, mitochondrial fragmentation and mitophagy. In summary, our data demonstrated that MitoQ treatment had a protective role in aortic fibrosis after PM<sub>2.5</sub> exposure through mitochondrial quality control, which regulated by mitochondrial ROS/PINK1/Parkin-mediated mitophagy. Our study provides a possible targeted therapy for PM<sub>2.5</sub>-induced arterial stiffness.

## 1. Introduction

Ambient particulate matter (PM) exposure is a serious public health problem concerning worldwide, and as reported it is the fourth leading risk factor for death in 2019, with more attributable deaths than high levels of low density lipoprotein cholesterol, high body mass index and alcohol consumption [1,2]. In 2017, there is also approximately 81% of the population in China who lived in regions where the air quality exceeded the World Health Organization (WHO) PM<sub>2.5</sub> transitional target I [3]. What's more, PM<sub>2.5</sub> is the lead environmental risk factor leading to the global mortality and disability rate of cardiovascular

diseases (CVDs) [4]. The increasing burden of CVDs makes it urgent to control cardiovascular risk factors and prevent CVDs [5–7]. Outdoor air pollution ranks fourth among preventable causes of disease burden in China [8]. However, the specific target of intervention is still ill-defined.

Accumulating epidemiological data have proved that short-term PM<sub>2.5</sub> exposure contributes to the occurrence and development of arteriosclerotic diseases such as hypertension, coronary heart diseases and peripheral artery diseases [4]. Vascular fibrosis serves on the key pathological process of vascular remodeling and involves excessive production and reduced degradation of extracellular matrix, which lie in the activation of phenotypic transformation of vascular smooth muscle

\* Corresponding author. Department of Toxicology and Sanitary Chemistry, School of Public Health, Capital Medical University, Beijing, 100069, PR China.

\*\* Corresponding author. Department of Toxicology and Sanitary Chemistry, School of Public Health, Capital Medical University, Beijing, 100069, PR China.

E-mail addresses: [jcduan@ccmu.edu.cn](mailto:jcduan@ccmu.edu.cn) (J. Duan), [zwsun@ccmu.edu.cn](mailto:zwsun@ccmu.edu.cn) (Z. Sun).

<https://doi.org/10.1016/j.redox.2021.102113>

Received 5 August 2021; Accepted 17 August 2021

Available online 18 August 2021

2213-2317/© 2021 The Authors.

Published by Elsevier B.V. This is an open access article under the CC BY-NC-ND license

(<http://creativecommons.org/licenses/by-nc-nd/4.0/>).

cells (VSMCs) [9,10]. VSMCs transform from contractile phenotype to synthetic phenotype in response to stressors and concomitant increase in the expression of synthetic markers such as osteopontin (OPN) [11]. The vulnerability of PM<sub>2.5</sub> to cardiovascular system may be correlated with its effect on vascular fibrosis, but there is a lack of study in this research area.

Mitochondria are sensitive targets of PM<sub>2.5</sub> as well as the main source of vascular oxidative stress that leads to arterial stiffness [12–14]. Mitochondrial quality control relies on mitochondrial dynamical homeostasis, which is continuously regulated by fission proteins (Dynamid-related protein 1, Drp1) and fusion proteins (Mitofusin-2, Mfn2) [15]. Dysfunctional mitochondria display membrane depolarization and fragmentation, accompanied by a large generation of mitochondrial reactive oxygen species and release of Ca<sup>2+</sup> into the cytoplasm in response to PM<sub>2.5</sub> exposure [16]. Cumulative studies suggest that vascular remodeling act as the product of mitochondrial oxidative stress as well as aberrant dynamics [17–19]. In addition, to prevent the vicious circle of mitochondrial damage and ROS production, cells protect themselves from mild damage depend on mitophagy, an inherent quality control mechanism [20]. It has reported that increased PINK1/Parkin-mediated mitophagy induced by PM<sub>2.5</sub> contributed to fibrosis in the liver and lung [21]. Excessive autophagy under stress was responsible for cardiac remodeling [22,23]. Thus, our study attempted to acquire a pharmacological approach to maintain mitochondrial quality control by targeting mitophagy for purpose of reducing PM<sub>2.5</sub>-related mitochondrial oxidative damage and protect against vascular injury.

The mitochondria-targeted antioxidant MitoQ is a derivative of coenzyme Q, which linked to TPP<sup>+</sup> by covalently binding to the 10-carbon aliphatic chain [24]. This lipophilic property makes it easier to cross biological membranes and gather in mitochondria with high concentration, which is equivalent to hundreds of times the effect of ordinary antioxidants [25]. Emerging studies indicated MitoQ exerted beneficial effects on diseases due to redox imbalance involved in cardiac fibrosis, contrast-induced kidney injury, COPD [26–28]. Clinical studies demonstrated that long-term oral MitoQ could improve vascular function in the elderly, which had been further verified in animal study that MitoQ treatment for 4 weeks in mice reduced the level of oxidative stress in aortic mitochondria and reversed the degree of aortic stiffness in aged mice [29,30]. Kang et al. suggested MitoQ protected against intervertebral disc degeneration through restoring mitochondrial dynamics imbalance and improving PINK-mediated mitophagy [31]. With respect to PM<sub>2.5</sub>-related vascular damage, the underlying mechanism remains unclear.

Our previous study proved that after the short-term PM<sub>2.5</sub> exposure ceases, the related vascular toxicity still persists for a long time in life, leading to the susceptibility of adult rats to arterial stiffness [32]. Similarly, the latest observations of WHO indicated that exposure to air pollution in childhood and adolescence changed the health trajectory of children as well as increased the risk of cardiovascular diseases such as hypertension later in life [33]. Thus it could be seen that the cardiovascular toxicity caused by air pollution may be more far-reaching and lasting than currently thought. Considering the above factors, we proposed whether MitoQ treatment could alleviate vascular injury and reduce the risk and burden of long-term cardiovascular disease in the future while short-term exposure to PM<sub>2.5</sub>. Therefore, the present study evaluated the effects of MitoQ on PM<sub>2.5</sub>-induced vascular damage of C57BL/6J mice, and verified the mechanism by which MitoQ regulated mitochondrial oxidative stress and dynamics and mitophagy in HAVSMCs.

## 2. Materials and methods

### 2.1. Preparation of PM<sub>2.5</sub> samples

PM<sub>2.5</sub> samples were collected by TH-1000C II high-flow atmospheric

particulate sampler (Wuhan Tianhong, China). PM<sub>2.5</sub> collected need to be eluted and lyophilized, and sterilized by UV before use. The morphology, particle size and composition of PM<sub>2.5</sub> samples used in this experiment have been measured in the previous study [34].

### 2.2. Experimental animal and treatment

A total of 72 seven-week-old male C57BL/6J mice were obtained from Vital River Laboratory Animal Technology Co., Ltd. (Beijing, China) and housed in the Experimental Animal Center of Capital Medical University. The animal experiment in this study was approved by the Animal Ethics Committee of Capital Medical University (Ethics No. AEEI-2016-076). After adaptive feeding for 1 week, C57 BL/6J mice were randomly divided into 4 groups: the Control group was given anhydrous ethanol dilution by gavage and saline by intratracheal instillation, the MitoQ group (5 mg/kg·bw) was given MitoQ by gavage and saline by intratracheal instillation, the PM<sub>2.5</sub> group (5 mg/kg·bw) was given anhydrous ethanol dilution by gavage and PM<sub>2.5</sub> suspension by intratracheal instillation, the MitoQ treated-PM<sub>2.5</sub> group was given MitoQ by gavage and PM<sub>2.5</sub> suspension by intratracheal instillation. The mice were given MitoQ gavage daily and PM<sub>2.5</sub> intratracheal instillation once every 3 days for 4 weeks.

MitoQ was purchased from MedChemExpress (MCE, China) and dissolved in anhydrous ethanol at 9:1 vol and diluted with normal saline when in use. The selection of PM<sub>2.5</sub> exposure dose was based on the interim target-1 35 µg/m<sup>3</sup> of the annual average concentration of PM<sub>2.5</sub> in the air quality guidelines recommended by the WHO, combined with the respiratory physiological parameters of mice, and the 100-fold uncertainty coefficient extrapolated by animals to the population.

### 2.3. Vascular Doppler ultrasound assessment

The vascular function and structure of mice were detected by the ultra-high resolution color Doppler ultrasound imaging system (Vevo 2100 Imaging System, FUJIFILM VisualSonics Inc., USA) after treatment. The mice were anesthetized by intraperitoneal injection of tribromoethanol which had little effect on heart rate to complete ultrasound examination. Aortic function indexes mainly include pulse wave velocity (PWV), left common carotid artery end diastolic velocity (LCCA EDV), left common carotid artery peak systolic velocity (LCCA PSV), as well as left common carotid artery pulsatility index (LCCA PI) and resistant index (LCCA RI) calculated from the above indicators, while carotid intima-media thickness (CIMT) was measured to evaluate aortic structure. All parameters need to be measured at least 3–5 cardiac cycles.

### 2.4. Histopathological analysis

The aortic tissue was isolated and collected after the mice were euthanized by cervical dislocation. Then part of the thoracic aorta was fixed with 4% paraformaldehyde for 24 h for purpose of histopathological analysis. Aorta segments were embedded with paraffin, sectioned at 5 µm pieces. The prepared paraffin sections of aorta were stained with hematoxylin and eosin (H&E) and verhoef's van gieson (EVG) to observe changes in histomorphology and elastic fibers. Besides, Masson's trichrome staining was conducted to evaluate aortic fibrosis. The slices were imaged by automatic slice scanning system (3Dhistech, Hungary).

### 2.5. Immunohistochemistry (IHC)

Paraffin slices were roasted, dewaxed in gradient, then repaired with antigen. After blocked with 10% fetal bovine serum for 1 h, the tissues were incubated with collagen I (1:100, Abcam, UK), OPN (1:200, Abcam, UK), Drp1 (1:100, CST, USA) at 4°C overnight and subsequently incubated with anti-rabbit IgG secondary antibody at 37°C for 30 min.

Thereafter, sections were stained with DAB. Images were acquired through automatic slice scanning system (3Dhitech, Hungary) and processed using Image-Pro Plus 6.0 software.

## 2.6. ROS in aorta detection

To evaluate reactive oxygen species (ROS) and mitochondrial ROS levels, the aorta tissues were prepared into frozen sections for DHE staining (BBoxiProbe, China) and MitoSOX staining (Invitrogen, USA) according to the manufacturer's protocols. Then sections were counterstained with 4',6-diamidino-2-phenylindole (DAPI). Fluorescence images were acquired using a confocal laser microscope (Nikon, Japan) and processed by Image J software.

## 2.7. Immunofluorescence

Frozen sections of aorta were permeated by 0.5% Triton X-100, blocked with 10% fetal bovine serum, and then co-incubated a-SMA (1:100, Abcam, UK) with OPN (1:100), SOD2 (1:100, Abcam, UK), PINK1 (1:100, Abcam, UK), Parkin (1:50, Novusbio, USA), as well as VDAC (1:200, Santa, USA) with LC3 (1:100, CST, USA) overnight at 4 °C, followed by incubation with a donkey anti-mouse Alexa Fluor 594-conjugated secondary antibody (1:200, Abcam, UK) and a goat anti-rabbit Dylight 488-conjugated secondary antibody (1:200, Abcam, UK) at 37 °C for 1 h. After DAPI staining was added to the sections, images were taken with the confocal laser microscope.

## 2.8. Cell culture and treatment

The human aortic vascular smooth muscle cell line (HAVSMC) was purchased from Shanghai Xinyu Biological Company. The cells were cultured in DMEM low-glucose medium (Gibco, USA) containing 10% bovine serum (Excell, Australia) and 1% penicillin streptomycin mixture at 37 °C under a 5% CO<sub>2</sub> atmosphere. Cells were incubated and converged to 70–80% density in the orifice plate before treatment. Does-dependent experiments were performed using 0–50 µg/mL PM<sub>2.5</sub> for 24 h. The HAVSMCs were pretreated with MitoQ (0.5 µM) for 2 h before exposure to 50 µg/mL PM<sub>2.5</sub>. PINK1 siRNA (20 µM) was pre-transfected into the HAVSMC using Lipofectamine™ 3000 (Invitrogen, USA) for 24 h in vitro studies.

## 2.9. Cell viability assay

The HAVSMCs were exposed to PM<sub>2.5</sub> at a series of concentrations (0, 12.5, 25, 50, 100 µg/mL) for 24 h. Then cell viability was measured by Cell Counting Kit-8 (CCK-8) kit (Tongren, Japan) according to the manufacturer's instruction.

## 2.10. ROS assessment

The generation of intracellular ROS and mitochondrial ROS were detected using CM-H<sub>2</sub>-DCFDA (Thermo, USA) and MitoSOX (Invitrogen, USA) fluorescent dyes. The cells after treatment were incubated with 5 µM CM-H<sub>2</sub>-DCFDA for 1 h or 5 µM MitoSOX for 15 min at 37 °C protected from light. After incubation, at least 1 × 10<sup>4</sup> cells were collected for flow cytometry analysis (Becton Dickinson, USA) of fluorescence intensity. Moreover, the living cells were also observed under the confocal laser microscope after subsequently stained with 1 µM Hoechst 33342 (Sigma, USA).

## 2.11. Ca<sup>2+</sup> levels measurement

The level of intracellular Ca<sup>2+</sup> was measured by Fluo-3 AM (Beyotime, China). After treatment, the HAVSMCs were incubated with 5 µM Fluo-3 AM for 30 min at 37 °C in dark. Then the Ca<sup>2+</sup> fluorescence intensity was evaluated using the flow cytometer and imaged under the

confocal laser microscope.

## 2.12. Mitochondrial membrane potential (MMP) determination

The influence on MMP was detected by JC-1 probe (Beyotime, China), which could selectively penetrate mitochondria and reversibly switch from red to green with decreased MMP. The HAVSMCs were incubated with 10 mg/L JC-1 for 20 min after treatment, then collected for flow cytometry analysis of red/green fluorescence intensity ratio as well as observed under the confocal laser microscope.

## 2.13. Mitochondrial oxygen consumption assay

The Mitochondrial oxygen consumption rate (OCR) is measured by Extracellular Oxygen Consumption Assay Kit (Abcam, UK) according to the manufacturer's protocol. In brief, the culture medium were replaced with 150 µL reaction medium for 30 min after the HAVSMCs were treated on 96-well cell culture plates. Then 10 µL oxygen consumption reagent and an oil layer were added to each well. Fluorescence was detected every 90 s for 90 min using a microplate reader (Thermo, USA) at 37 °C.

## 2.14. ATP measurement

ATP was assayed using the ATP determination kit (Invitrogen, USA) by a coupled luciferin/luciferase reaction. The HAVSMCs were lysed by 10 µL lysis buffer for 30 min after treatment on 96-well culture plates. 100 µL working solution were added and incubated for 15 min. The fluorescence was measured at 560 nm.

## 2.15. Cell ultrastructural observation

The HAVSMCs were harvested to prefix in 2.5% glutaraldehyde, and then samples were prepared after fixation, dehydration and embedding, sections were observed under a transmission electron microscope (TEM, HT7700, Japan).

## 2.16. Cell immunofluorescence

The HAVSMCs were cultivated on cell slices in 12-well plates for staining. After treatment, cells were fixed by 4% paraformaldehyde for 15 min, followed by permeabilized with 0.1% Triton X-100 for 5 min, and then 10% fetal bovine serum was used to block nonspecific binding sites. The cell slides were co-incubated VDAC (1:200) with Drp1 (1:50), LC3 (1:50), Parkin (1:50) at 4 °C overnight. After incubating with secondary antibody for 1 h and staining with DAPI, the images were obtained by confocal laser microscope.

## 2.17. Western blot assay

Total protein were isolated from aortic tissue and the HAVSMCs using total protein extraction kit (key Gen, China) and quantified by BCA protein assay (Dingguo, China). 40 µg of protein samples were separated using 12% SDS-PAGE and transferred to nitrocellulose membranes, which were probed with primary and then corresponding secondary antibodies. The protein bands were detected by Image Lab™ software (Bio-Rad, USA) and analysed using Image J software.

## 2.18. Statistical analysis

Statistical analysis was conducted by GraphPad Prism 5.0 software. All data were expressed as mean ± S.D. Student's t-test was used to compare the data of two groups, and one-way ANOVA was used to compare the data of three groups and more. *p* < 0.05 was considered statistically significant.

### 3. Results

#### 3.1. Effects of MitoQ on vascular function and structure alterations in PM<sub>2.5</sub>-exposed mice

Vascular Doppler ultrasound imaging system showed the changes of aortal changes of mice (Fig. 1A). PM<sub>2.5</sub>-exposed mice exhibited notably faster PWV, lower LCCA EDV, higher LCCA PI and RI compared to the control mice, while lower PWV, increased LCCA EDV, decreased LCCA PI and RI were observed in PM<sub>2.5</sub>-exposed mice after MitoQ treatment (Fig. 1B, 1D, 1F, 1G). But no obvious variation on LCCA PSV was found among the different groups (Fig. 1E). Besides, we also detected aortal structure via CIMT indicator, PM<sub>2.5</sub>-exposed mice showed increased CIMT, which were decreased after MitoQ treatment (Fig. 1C). These results indicated that short-term PM<sub>2.5</sub> exposure could cause systolic and diastolic dysfunction of aorta and structural damage such as wall thickening in mice which could be improved after MitoQ treatment, suggesting that MitoQ alleviated aortic stiffness induced by PM<sub>2.5</sub>.

#### 3.2. MitoQ attenuated PM<sub>2.5</sub>-induced pathologic injury and fibrosis of aorta

H&E staining displayed that the media membrane of aorta wall in mice exposed to PM<sub>2.5</sub> was thickened, and SMCs were hyperplasia and disorderly arranged compared with the control mice. Meanwhile, the elastic fibers of aorta in PM<sub>2.5</sub> group were broken, tortuous and loosely arranged versus the control mice by EVG staining, whereas MitoQ treatment reversed these changes (Fig. 2A and B). Besides, Masson's staining showed the fibrotic area increased in PM<sub>2.5</sub>-exposed aorta

compared with the control and this was attenuated by MitoQ (Fig. 2C). To further verify the effect on aortic fibrosis, we also detected the expression level of collagen in aorta. IHC staining and Western blot assay of collagen I revealed a marked increase in its expression in the aorta of PM<sub>2.5</sub>-exposed mice, and MitoQ significantly restored this change, likewise the expression level of collagen III was enhanced in the aorta of PM<sub>2.5</sub>-exposed mice while MitoQ reduced its expression (Fig. 2D, 2G, 2H). Fibrosis development involves the switch of SMCs into synthetic phenotype. Here we measured the expression level of OPN in aorta, which is a key marker of synthetic SMCs. IHC showed notably increased OPN expression in aorta of PM<sub>2.5</sub>-exposed mice compared to the control, and MitoQ reversed this change, meanwhile, immunofluorescence collocation staining showed an increased expression of OPN in a-SMA-marked VSMCs in PM<sub>2.5</sub>-exposed mice while MitoQ reversed this change, and the results were further confirmed by Western blot (Fig. 2E-G, 2I). These results suggested that MitoQ could alleviate aortic fibrosis and phenotypic transformation of SMCs induced by PM<sub>2.5</sub>.

#### 3.3. Effect of MitoQ on mitochondrial oxidative stress and mitochondrial dynamic homeostasis in PM<sub>2.5</sub>-exposed mice

Oxidative stress plays a crucial role in PM<sub>2.5</sub>-mediated vascular toxicity. Fluorescence staining demonstrated the production of ROS in the aorta of mice exposed to PM<sub>2.5</sub> was significantly increased while MitoQ administration reversed this change (Fig. 3A and a). Mitochondria play an inescapable role in oxidative stress, so we further evaluated the level of mitochondrial oxidative stress, MitoSOX staining showed the mitochondrial ROS level in the aorta was significantly increased in PM<sub>2.5</sub>-exposed mice, and MitoQ markedly decreased the PM<sub>2.5</sub>-induced

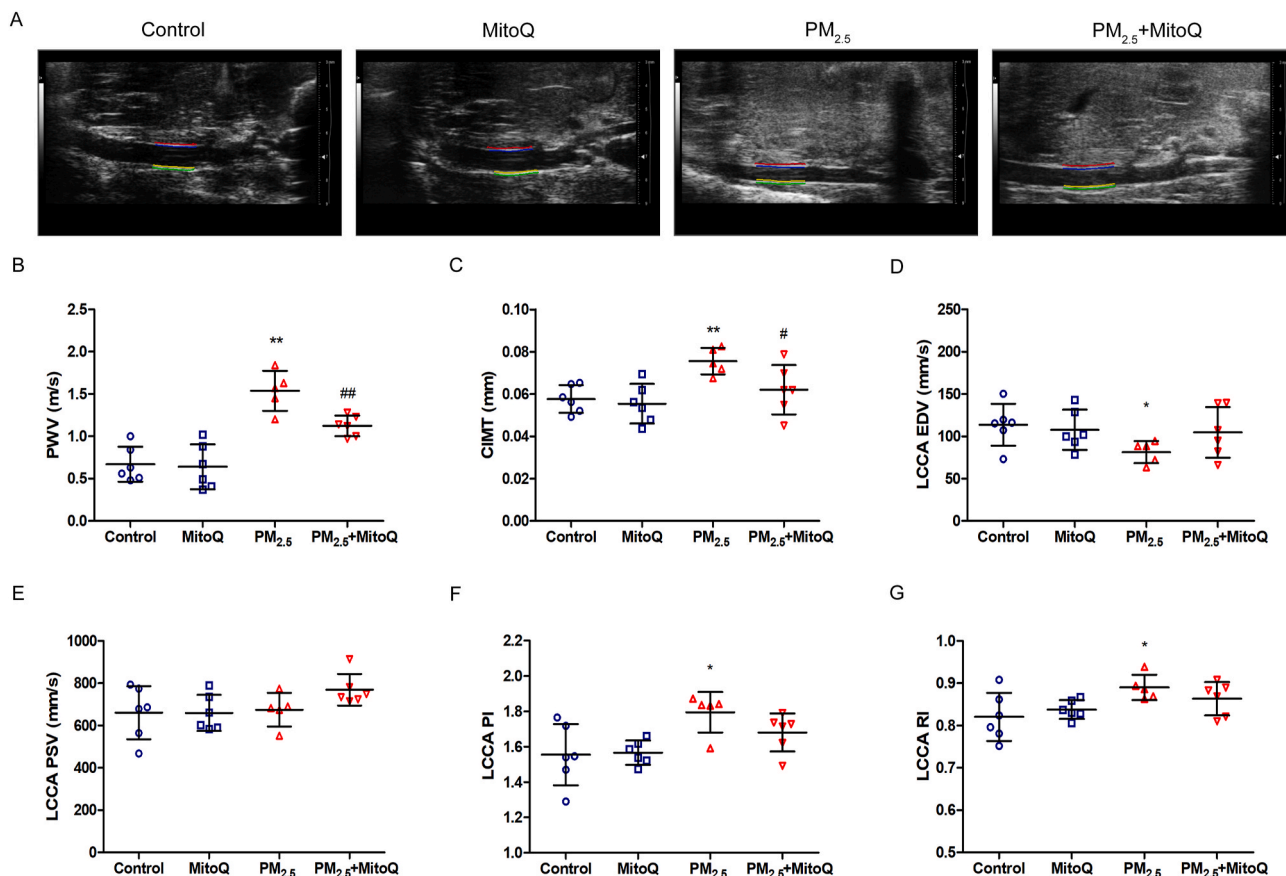
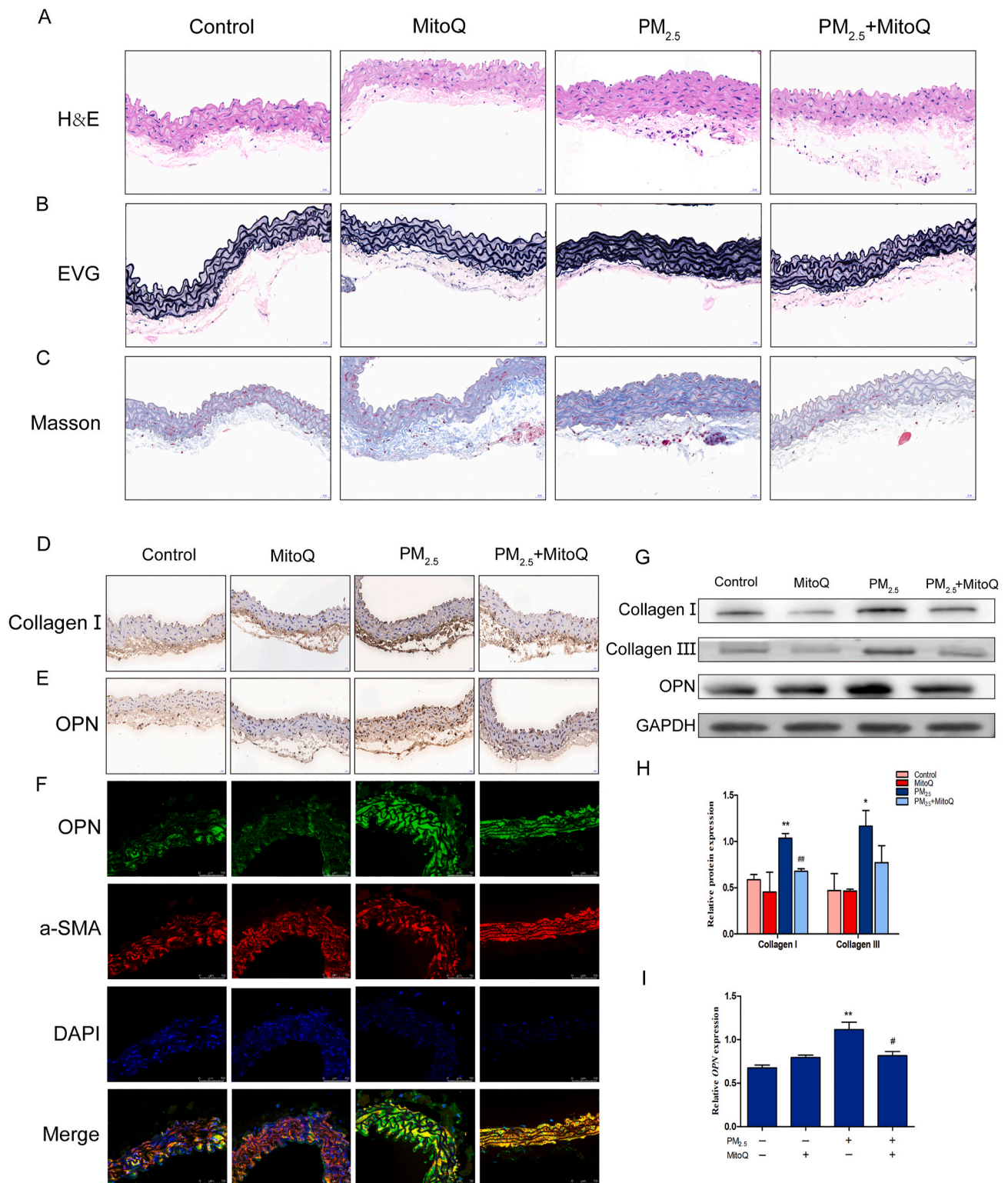


Fig. 1. Effects of MitoQ on PM<sub>2.5</sub>-induced aortic dysfunction and structure alterations in C57BL/6J mice. (A), Vascular Doppler ultrasound images. (B), PWV. (C), CIMT. (D), LCCA EDV. (E), LCCA PSV. (F), LCCA PI. (G) LCCA RI. \* represents compared to the control group, # represents compared to the PM<sub>2.5</sub> group. \**p* < 0.05, \*\**p* < 0.01, ##*p* < 0.01.



**Fig. 2.** MitoQ attenuated histopathological changes and fibrosis of aorta in PM<sub>2.5</sub>-exposed C57BL/6J mice. (A), H&E staining. (B), EVG staining. (C), Masson's trichrome staining. (D), The IHC staining of collagen I. (E), The IHC staining of OPN. Scale bar: 20  $\mu$ m. (F), IF double-staining of a-SMA and OPN. Scale bar: 50  $\mu$ m (G–I), Western blot assay showed the expression of collagen I, collagen III, OPN and quantitative analysis. \* represents compared to the control group, # represents compared to the PM<sub>2.5</sub> group. \**p* < 0.05, \*\**p* < 0.01, #*p* < 0.05, ##*p* < 0.01.

mitochondrial ROS level (Fig. 3B and b). Meanwhile, SOD2 expression was found to be unexpectedly up-regulated in a-SMA marked VSMCs in PM<sub>2.5</sub>-exposed mice compared to those of the control by fluorescence staining, and its expression level was further increased after MitoQ treatment (Fig. 3C and c). In addition, we also evaluated mitochondrial

dynamics-related proteins, IHC staining showed Drp1 expression was up-regulated in aorta of PM<sub>2.5</sub>-exposed mice compared to the control mice, while Mfn2 expression was down-regulated detected by Western blot assay. And MitoQ treatment partially reduced Drp1 expression and restored Mfn2 expression in PM<sub>2.5</sub>-exposed mice (Fig. 3D - e). These

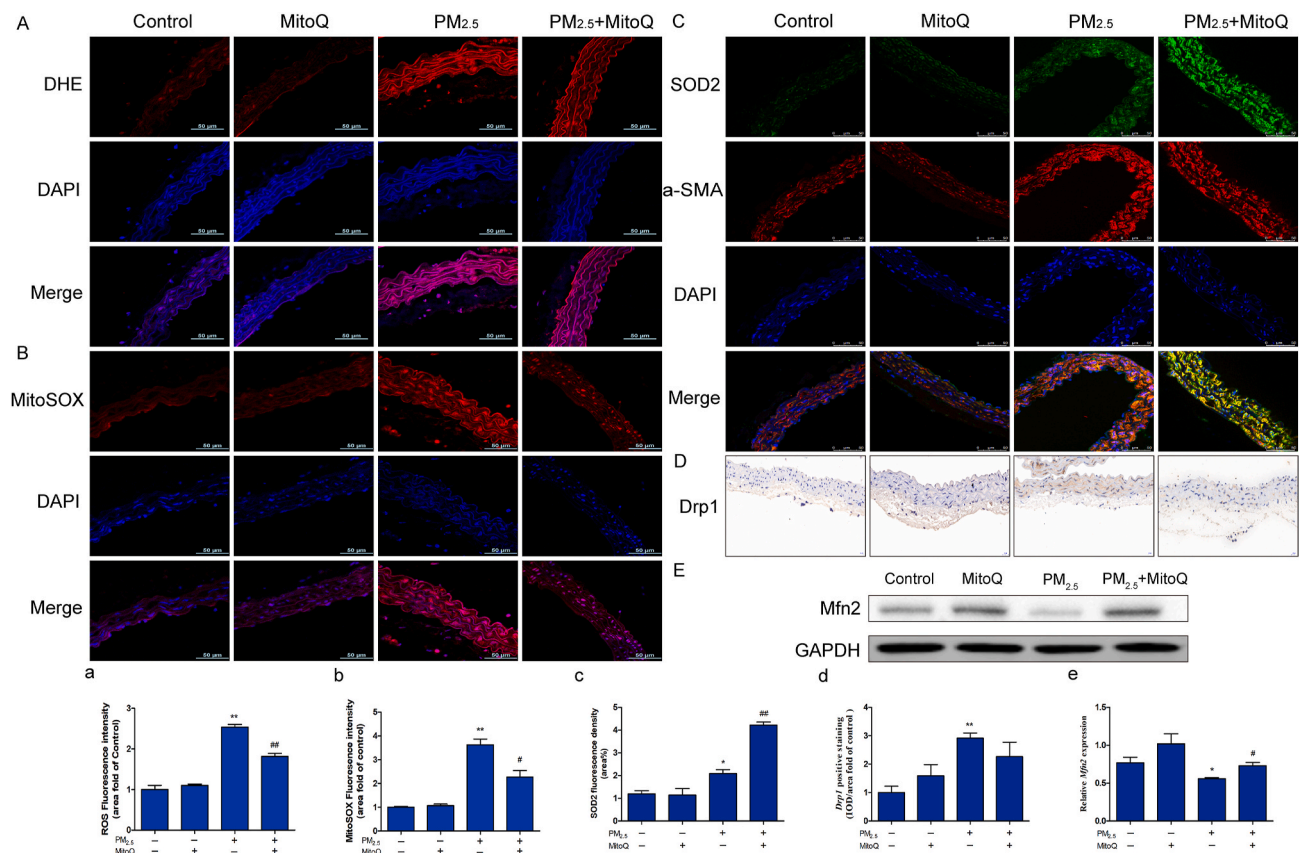


**Fig. 3.** Effect of MitoQ on mitochondrial oxidative stress and mitochondrial dynamic homeostasis in PM<sub>2.5</sub>-exposed aorta. (A and a), DHE staining of aorta tissues and the quantitative analysis of ROS fluorescence intensity. (B and b), MitoSOX staining of aorta tissues and the quantitative analysis of mitochondrial ROS fluorescence intensity. (C and c), The IF double-staining of a-SMA and SOD2 and the quantitative analysis of SOD2 fluorescence intensity. Scale bar: 50  $\mu$ m. (D and d), The IHC staining of Drp1 and quantitative analysis. Scale bar: 20  $\mu$ m. (E and e), Western blot assay showed the expression of Mfn2 and quantitative analysis. \* represents compared to the control group, # represents compared to the PM<sub>2.5</sub> group. \* $p$  < 0.05, \*\* $p$  < 0.01, # $p$  < 0.05, ## $p$  < 0.01.

results indicated MitoQ might act a part in mitochondrial quality control by improving aortal oxidative stress in PM<sub>2.5</sub>-exposed mice.

### 3.4. Effect of MitoQ on mitophagy in VSMCs of PM<sub>2.5</sub>-exposed mice

Immunofluorescence co-location staining of LC3 revealed PM<sub>2.5</sub> notably elevated its expression in VDAC-marked mitochondria of aorta, and MitoQ partially reversed this change. Meanwhile, immunoblotting also showed LC3II/I ratio and p62 expression were markedly up-regulated in PM<sub>2.5</sub>-exposed mice, and MitoQ treatment partially inhibited these effects (Fig. 4A and 4D), indicating MitoQ intervention attenuated mitophagy activated by PM<sub>2.5</sub> exposure in aortic tissue. Mitophagy mainly depends on the regulation of PINK1/Parkin signal pathway. Fluorescence images showed PINK1 and Parkin colonization in the VSMCs of mice, increased PINK1 and Parkin green intensity were observed in PM<sub>2.5</sub>-exposed mice compared to the control mice, while these changes were notably decreased after MitoQ treatment (Fig. 4B and 4C). Moreover, the similar results were again confirmed by immunoblotting (Fig. 4D). The above results proved that MitoQ attenuated the PINK1/Parkin-dependent mitophagy pathway in aorta activated by PM<sub>2.5</sub> exposure.

### 3.5. PM<sub>2.5</sub> induced mitochondrial dysfunction and phenotypic switch in HAVSMCs

As shown in Fig. 5A, the HAVSMCs viability increased first and then decreased with the increase of PM<sub>2.5</sub> concentration and the cell viability in the 50  $\mu$ g/mL dose group was significantly higher than that in the control group while dropped markedly in the 100  $\mu$ g/mL. Considering

that the dose of PM<sub>2.5</sub> (100  $\mu$ g/mL) may be overdosed, we chose the concentration range of PM<sub>2.5</sub> between 0 and 50  $\mu$ g/mL in the following experiments. The intracellular Ca<sup>2+</sup> content enhanced continuously with the increase of PM<sub>2.5</sub> exposure concentration measured by flow cytometer analysis, which indicated that PM<sub>2.5</sub> triggered the Ca<sup>2+</sup> imbalance in HAVSMCs (Fig. 5B and b). Fluorescence staining manifested a gradually elevated ROS (green) and mitochondrial ROS (red) fluorescence as the increasing dose of PM<sub>2.5</sub>, and the further flow quantitative analysis of fluorescence intensity showed a dose-dependent increase of ROS and mitochondrial ROS after PM<sub>2.5</sub> exposure (Fig. 5C–f). Immunoblotting assay detected proteins related to mitochondrial quality control in HAVSMCs (Fig. 5G–P), increased expression levels of Drp1 and SOD2 while decreased Mfn2 were observed in HAVSMCs, dose-dependent changes induced by PM<sub>2.5</sub> exposure. In addition, the expression levels of LC3II/I, p62 and PINK1 were gradually elevated in HAVSMCs with increasing PM<sub>2.5</sub> dose while there was no obvious change about Parkin. Regarding the effect of HAVSMCs phenotype switch, PM<sub>2.5</sub> increased the expression levels of collagen I and OPN proteins in a dose-dependent manner. Taken together, PM<sub>2.5</sub> induced mitochondrial oxidative stress, mitochondrial dynamics imbalance and activated mitophagy, as well as synthetic phenotype remodeling in HAVSMCs.

### 3.6. Effect of MitoQ on mitochondrial dysfunction in HAVSMCs subjected to PM<sub>2.5</sub> exposure

MitoSOX staining displayed elevated mitochondrial ROS levels in HAVSMCs exposed to PM<sub>2.5</sub> conditions while MitoQ treatment reversed this change, and the further flow quantitative analysis of fluorescence

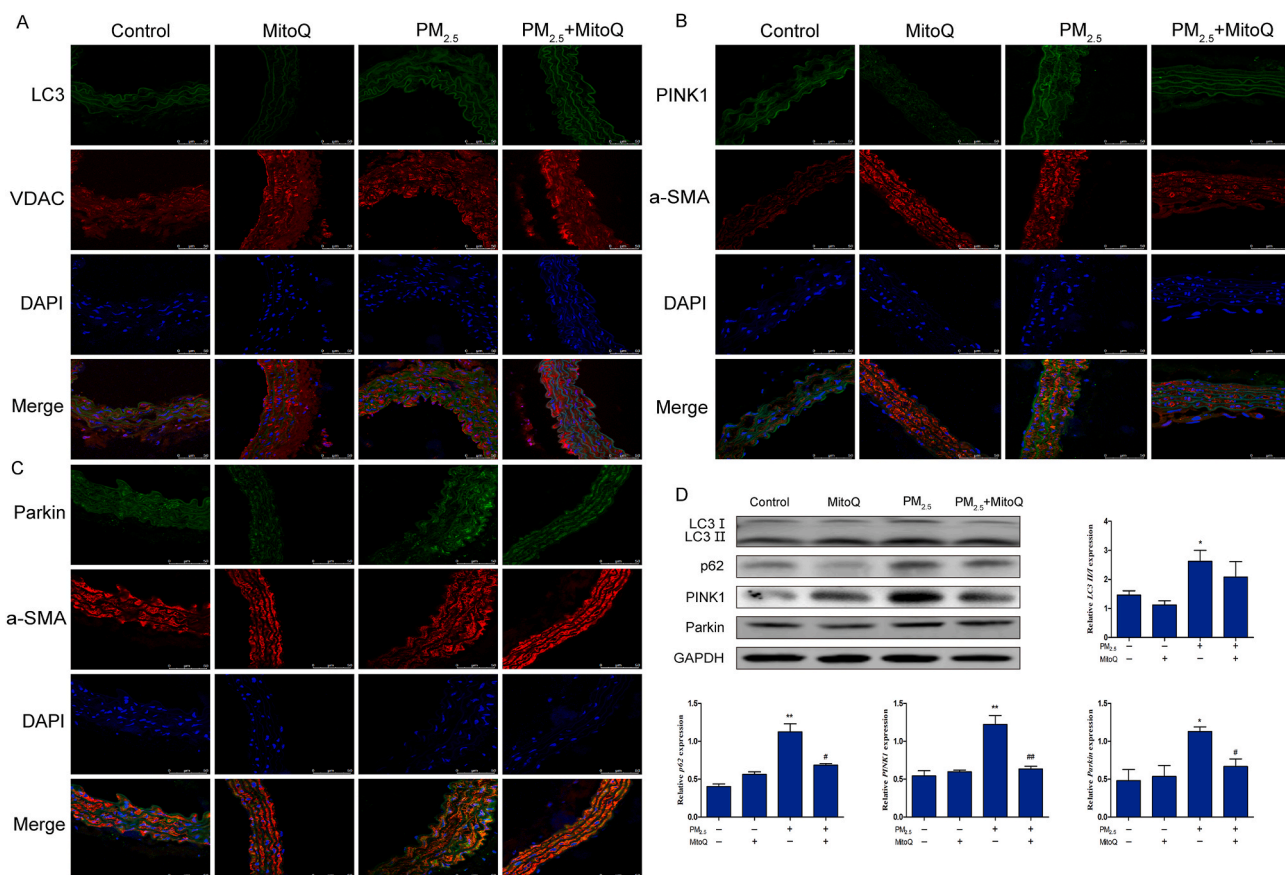


**Fig. 4.** Effect of MitoQ on PM<sub>2.5</sub>-induced mitophagy in VSMCs of aorta. (A), The IF double-staining of LC3 and VDAC. (B–C), The IF double-staining of a-SMA and PINK, Parkin. (D), Western blot assay showed the protein expression of LC3, p62, PINK, Parkin and quantitative analysis. Scale bar: 50  $\mu$ m \* represents compared to the control group, # represents compared to the PM<sub>2.5</sub> group. \* $p$  < 0.05, \*\* $p$  < 0.01, # $p$  < 0.05, ## $p$  < 0.01. (For interpretation of the references to color in this figure legend, the reader is referred to the Web version of this article.)

intensity also revealed MitoQ markedly decreased the mitochondrial ROS levels in HAVSMCs exposed to PM<sub>2.5</sub> (Fig. 6A - b). Meanwhile, fluorescence staining and flow cytometry analysis demonstrated MitoQ obviously reduced the enhanced intracellular Ca<sup>2+</sup> levels induced by PM<sub>2.5</sub> (Fig. 6C - d). As shown in Fig. 6F, increased green intensity and decreased red intensity were observed in PM<sub>2.5</sub>-exposed HAVSMCs, while MitoQ treatment partially reversed reduced MMP induced by PM<sub>2.5</sub>. Meanwhile, the flow quantitative analysis of the red/green ratio further demonstrated the above results (Fig. 6E). Besides, MitoQ also obviously reversed the reduced OCR and ATP synthesis in PM<sub>2.5</sub>-exposed HAVSMCs (Fig. 6G and H). TEM revealed that most mitochondria in control HAVSMCs exhibited slender cylindrical shape, while fragmented mitochondria and increased mitochondrial autophagosomes were observed after PM<sub>2.5</sub> exposure. However, MitoQ partially reversed this effect (Fig. 6I). Double immunofluorescence staining showed MitoQ treatment obviously reduced the Drp1 intensity in VDAC-marked mitochondria of HAVSMCs after PM<sub>2.5</sub> exposure, and similar results were also observed via immunoblotting (Fig. 7A–C). MitoQ partially reversed the decrease in Mfn2 expression in PM<sub>2.5</sub>-exposed HAVSMCs as shown by immunoblotting (Fig. 7B and D). These data revealed MitoQ partially restored mitochondrial dysfunction induced by PM<sub>2.5</sub> in HAVSMCs.

### 3.7. Effect of MitoQ on mitophagy and phenotypic switch in PM<sub>2.5</sub>-exposed HAVSMCs

Immunofluorescence double staining was performed to evaluate the effect on mitophagy, increased LC3 intensity and Parkin intensity in VDAC-marked mitochondria were observed after PM<sub>2.5</sub> exposure as

MitoQ treatment partially reversed this effect, meanwhile, immunoblotting also manifested the similar results that PM<sub>2.5</sub> exposure notably increased the expression levels of LC3II/I, PINK1, Parkin and p62 in HAVSMCs while MitoQ treatment partially decreased these effects (Fig. 7E–G, 7J–M). And as for phenotypic switch, immunoblotting assay also revealed MitoQ significantly down-regulated the expression levels of collagen I and OPN induced by PM<sub>2.5</sub> (Fig. 7G–I).

### 3.8. MitoQ restored mitophagy and synthetic phenotype in PM<sub>2.5</sub>-exposed HAVSMCs partially via PINK1

PINK1 siRNA was used to detect how PINK1 regulate the effects of MitoQ on HAVSMCs under PM<sub>2.5</sub> exposure (Fig. 8). Western blot assay revealed the expression level of OPN was notably increased in PM<sub>2.5</sub>-exposed HAVSMCs but was partially restored by PINK1 siRNA transfection after MitoQ treatment. Meanwhile, immunoblotting also demonstrated that PM<sub>2.5</sub>-induced increases in Drp1 and decreases in Mfn2 expression were restored after MitoQ treatment, while these changes were partially abolished by PINK1 siRNA transfection. Besides, PM<sub>2.5</sub>-enhanced LC3II/I, p62, PINK1 and Parkin expression levels were removed after MitoQ treatment and were further restored by PINK1 siRNA transfection. These results indicated that MitoQ mediated mitochondrial quality control and synthetic phenotype of HAVSMCs under PM<sub>2.5</sub> exposure partially via PINK1.

## 4. Discussion

In recent years, the burden of cardiovascular diseases caused by ambient PM<sub>2.5</sub> has continued to increase, and the profound impact of

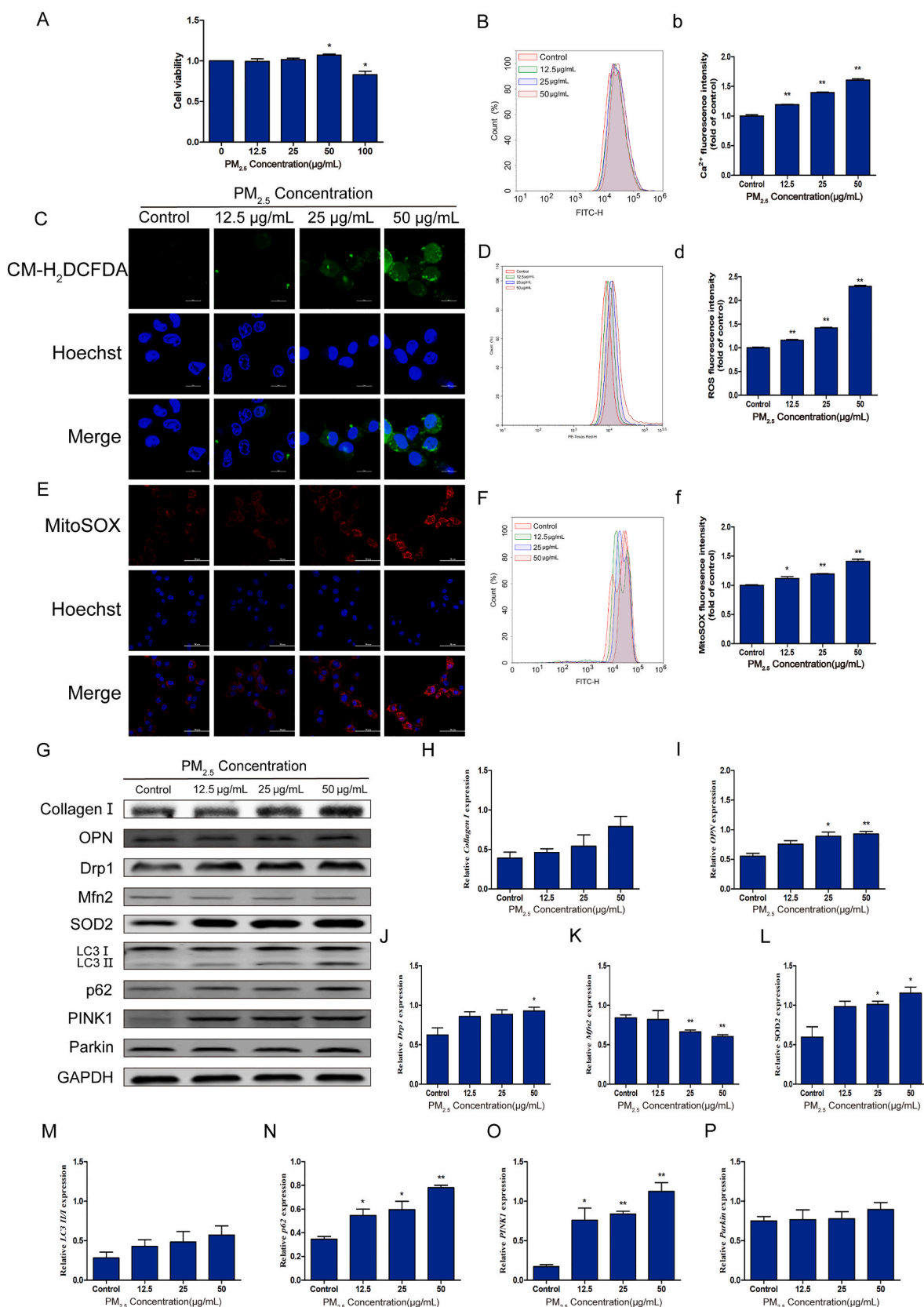


**Fig. 5.** PM<sub>2.5</sub> induced mitochondrial dysfunction and synthetic phenotype remodeling in HAVSMCs. (A), The cell viability of PM<sub>2.5</sub>-exposed HAVSMCs. (B and b), The quantitative analysis of Ca<sup>2+</sup> by flow cytometry. (C), Staining of ROS in HAVSMCs. Scale bar: 10 μm. (D and d), The quantitative analysis of ROS by flow cytometry. (E), Staining of mitochondrial ROS in HAVSMCs. Scale bar: 50 μm. (F and f), The quantitative analysis of mitochondrial ROS by flow cytometry. (G–P), Western blot assay showed the protein expression of collagen I, OPN, Drp1, Mfn2, SOD2, LC3, p62, PINK1, Parkin and quantitative analysis. \* represents compared to the control group, # represents compared to the PM<sub>2.5</sub> group. \**p* < 0.05, \*\**p* < 0.01, #*p* < 0.05, ##*p* < 0.01. (For interpretation of the references to color in this figure legend, the reader is referred to the Web version of this article.)



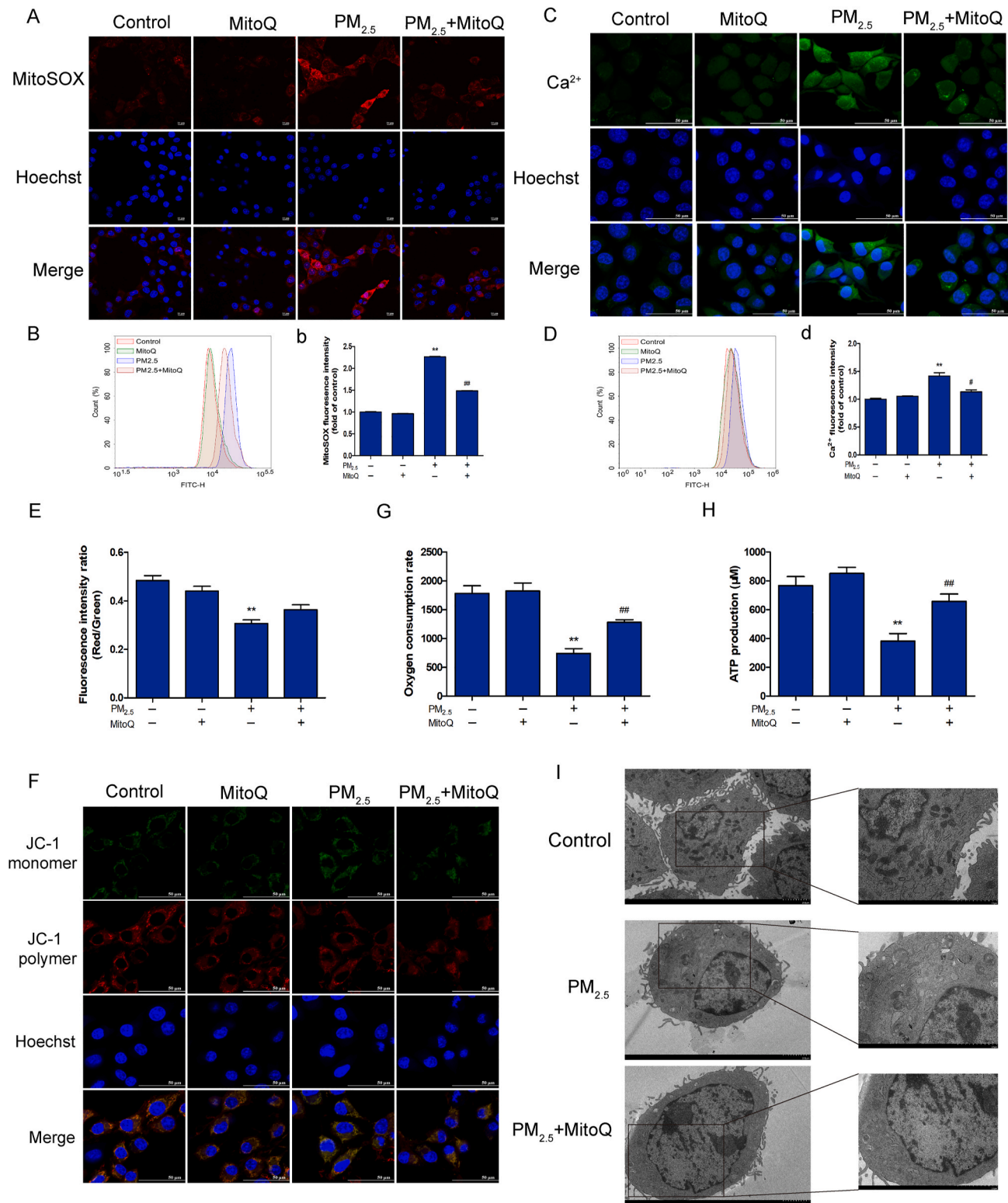


**Fig. 6.** Effect of MitoQ on mitochondrial dysfunction in PM<sub>2.5</sub>-exposed HAVSMCs. (A), Staining of mitochondrial ROS in HAVSMCs. Scale bar: 10 μm. (B and b), The quantitative analysis of mitochondrial ROS by flow cytometry. (C), Staining of Ca<sup>2+</sup> in HAVSMCs. Scale bar: 50 μm. (D and d), The quantitative analysis of Ca<sup>2+</sup> by flow cytometry. (E), The quantitative analysis of MMP in HAVSMCs by flow cytometry. (F), Fluorescence staining of MMP. Scale bar: 50 μm. (G), The measurement of oxygen consumption rate in HAVSMCs. (H), The ATP production detection. (I), TEM images showed mitophagy. Scale bar: 2.0 μm \* represents compared to the control group, # represents compared to the PM<sub>2.5</sub> group. \**p* < 0.05, \*\**p* < 0.01, #*p* < 0.05, ##*p* < 0.01.

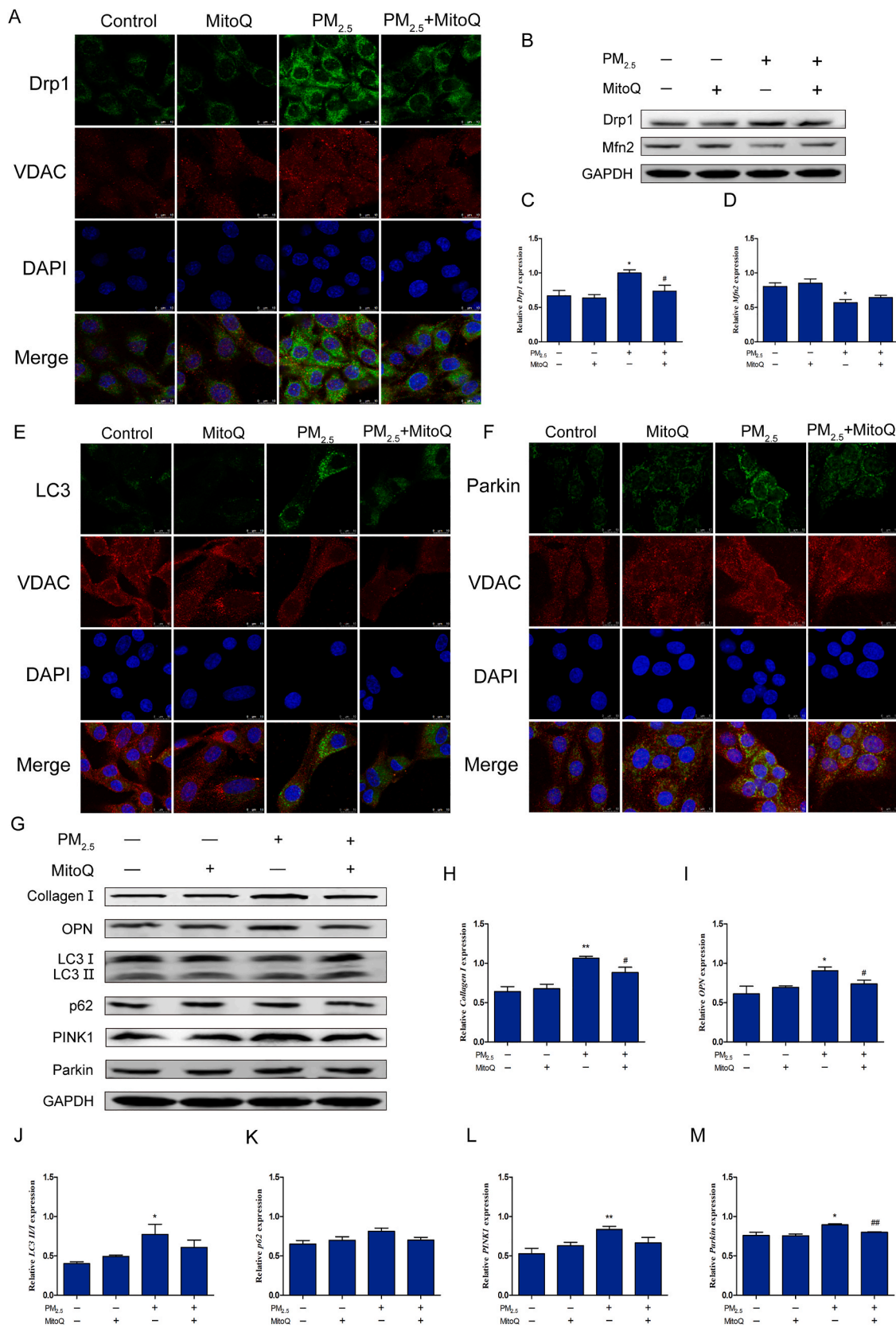


**Fig. 7.** MitoQ restored mitophagy and synthetic phenotype in PM<sub>2.5</sub>-exposed HAVSMCs via PINK1. (A), IF double-staining of Drp1 and VDAC. Scale bar: 10 μm. (B–D), Western blot assay showed the protein expression of Drp1, Mfn2 and quantitative analysis. (E and F), IF double-staining of VDAC and LC3, Parkin. Scale bar: 10 μm. (G–M), Western blot assay showed the protein expression of collagen I, OPN, LC3, p62, PINK1, Parkin and quantitative analysis. \* represents compared to the control group, # represents compared to the PM<sub>2.5</sub> group. \**p* < 0.05, \*\**p* < 0.01, #*p* < 0.05, ##*p* < 0.01. (For interpretation of the references to color in this figure legend, the reader is referred to the Web version of this article.)

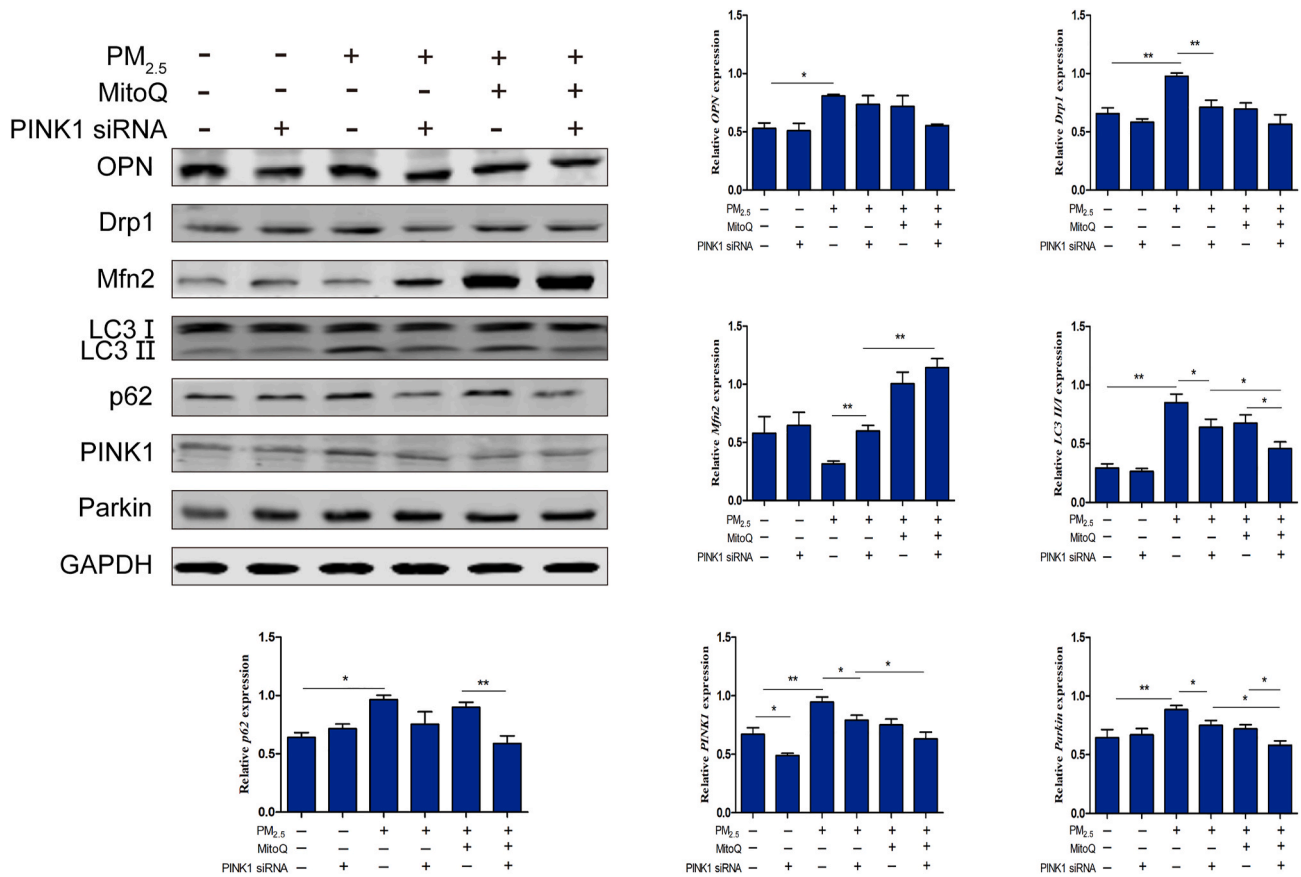


**Fig. 8.** MitoQ restored mitophagy and synthetic phenotype in PM<sub>2.5</sub>-exposed HAVSMCs via PINK1. Western blot assay showed the effect of PINK1 siRNA on the protein expression of OPN, Drp1, Mfn2, LC3, p62, PINK1, Parkin and quantitative analysis. \* represents compared to the control group, # represents compared to the PM<sub>2.5</sub> group. \**p* < 0.05, \*\**p* < 0.01, #*p* < 0.05, ##*p* < 0.01. (For interpretation of the references to color in this figure legend, the reader is referred to the Web version of this article.)

short-term PM<sub>2.5</sub> exposure on cardiovascular risk has attracted more and more attention. Increasing studies are focused on the anti-damage research caused by PM<sub>2.5</sub> [35,36]. In our study, we elucidated aortic fibrosis due to short-term PM<sub>2.5</sub> exposure, and revealed for the first time that the protective role of MitoQ depended on mitochondrial ROS/PINK1/Parkin-mediated mitophagy which involving phenotypic transformation of HAVSMCs.

PM<sub>2.5</sub> exposure can cause changes in subclinical indexes of cardiovascular function. PWV is the gold standard used for evaluating arterial stiffness [37]. The reduction of hemodynamic parameters PSV and EDV indicates mild carotid artery stenosis, which is independently correlated with the occurrence of future cardiovascular events, as well as PI and RI are markers of arterial resistance and compliance [38,39]. In current study, PM<sub>2.5</sub> exposure induced enhanced PWV, slowed blood flow and increased arterial resistance, which reflected aortic dysfunction and ultimately led to arterial stiffness (Fig. 1). In individuals with aortic sclerosis, the blood flow pressure waves return and enter the systole faster than normal, increasing cardiac afterload which induced left ventricular hypertrophy, and reducing coronary blood flow, leading to myocardial hypoperfusion and may cause myocardial ischemia and heart failure [40]. Besides, aortic stiffness is also the precursor to hypertension [41]. A population study showed short-term PM<sub>2.5</sub> exposure caused ankle-arm PWV to increase in healthy subjects, which is consistent with our results [42]. Similarly, a cohort study reported that short-term PM<sub>2.5</sub> exposure caused acute cerebrovascular events related to increased cerebrovascular resistance and reduced cerebral blood flow velocity [43]. Additionally, our data indicated PM<sub>2.5</sub> exposure induced increased CIMT, suggesting aortic function and structure could be changed by short-term PM<sub>2.5</sub> exposure.

The mechanical properties of aorta depend to a large extent on its structural rigidity, which is related to the fibrous extracellular matrix component of the vessel wall, involving structural proteins (collagen and elastin) and adhesion proteins (such as laminin and fibronectin) [44]. The broken elastic fibers in our study also confirmed this point (Fig. 2). Besides, vascular fibrosis is largely due to increased deposition of collagen I and collagen III in the vessel wall and perivascular areas, which can alter the passive pressure/diameter relationship of artery under higher pressure and induce a gradual hardening of vessel wall [11, 45]. As expected, PM<sub>2.5</sub> caused the deposition of collagen I and collagen III in aorta, and the fibrosis was obvious in our study (Fig. 2). It has been reported that increased aortic collagen deposition was observed in C57BL/6J mice after PM exposure 1 month [46], which supported our results. Importantly, we have further refined the mechanism of PM<sub>2.5</sub> related aortic fibrosis in vivo and in vitro that VSMCs transformed into a synthetic phenotype in response to PM<sub>2.5</sub> treatment, which expressed OPN protein and secreted extracellular matrix such as collagen I (Figs. 2 and 5). However, the pathogenesis underlying the phenomena is not fully understood.

Our previous study and others have certified mitochondrial dysfunction is mainly responsible for PM<sub>2.5</sub> induced CVDs [47,48]. Mitochondrial redox state unbalance plays a vital role in phenotypic regulation of VSMCs [49]. In present study, we found PM<sub>2.5</sub> exposure caused mitochondrial ROS overproduction and elevated SOD2 expression (Figs. 3 and 5). The body's antioxidant system will be activated to resist the increase of oxidative stress and protect tissues from damage in response to PM<sub>2.5</sub> exposure, while SOD2 plays a central role in this process [50]. Meanwhile, decreases in MMP, OCR and ATP synthesis, increases in intracellular Ca<sup>2+</sup> and mitochondrial fragmentation have

also been triggered after PM<sub>2.5</sub> exposure in this study (Figs. 5 and 6). These results coincided with our previous study involving PM<sub>2.5</sub>-exposed BEAS-2B cells [16]. ROS/Drp1-regulated mitochondrial fragmentation was involved in the VSMC synthetic phenotype remodeling, which may be a target for the treatment of proliferative vascular diseases [17,51]. Marsboom et al. found that activated Drp1 was induced in the pulmonary blood vessels of patients with idiopathic pulmonary hypertension, and inhibiting excessive mitochondrial division could reduce proliferation of pulmonary artery smooth muscle cells as well as pulmonary hypertension [52]. But, whether inhibition of mitochondrial ROS overproduction can reverse VSMCs synthetic phenotype remodeling induced by PM<sub>2.5</sub> through mitochondrial quality control remains unclear.

Antioxidants maintain cell redox homeostasis to eliminate potential damage. However, conventional antioxidant therapies lack specificity and cannot reach effective concentrations at the site of pathological oxidative stress, while MitoQ can just overcome the shortcoming [53]. A certain accumulation of MitoQ was detected in the heart and vessel of rats after oral intervention [54]. In a clinical study, 20 healthy elderly patients with impaired endothelial function decreased cervical-femoral PWV, increased brachial artery flow-mediated dilatation, as well as decreased aortic stiffness after 6 weeks of oral MitoQ (20 mg/d), which was expected to treat vascular dysfunction caused by ageing [29]. MitoQ inhibited the interaction between TGF- $\beta$ 1 and mitochondria-related redox signaling to improve cardiac hypertrophic remodeling, fibrosis and left ventricular dysfunction in mice [26]. Interestingly, we also found MitoQ reversed aortic stiffness and histological changes, especially as for fibrosis and VSMCs synthetic phenotype remodeling induced by PM<sub>2.5</sub> in current study (Figs. 1, 2 and 7). However, the superiority of MitoQ in treating PM<sub>2.5</sub>-related vascular injury needed more cohort study to conduct on this issue.

Regarding to the protective effect of MitoQ on mitochondrial dysfunction induced by PM<sub>2.5</sub>, we found that mitochondrial oxidative stress, decreased MMP, OCR and ATP synthesis, increased Ca<sup>2+</sup> amendment were accompanied by alleviated mitochondrial fragmentation after MitoQ treatment (Figs. 3, 6 and 7). Similarly, Yang et al. believed that MitoQ treatment attenuated oxidative stress, decreased Drp1 expression and increased Mfn2 expression in lung induced by cigarette smoke [55]. Increased mitochondrial fragmentation initiates mitophagy to clear damaged mitochondria, thus maintaining mitochondrial quality control and function [56]. As expected, PM<sub>2.5</sub> exposure increased mitophagy in aorta and HAVSMCs (Figs. 4–6). Environmental exposure may cause airway epithelial cells to produce ROS, which activates autophagy pathways, leading to phenotypic changes and fibrosis of airway remodeling [57], which is consistent with our study. But there is limited study focused on the role of mitophagy in PM<sub>2.5</sub>-related vascular injury, as well as whether targeting mitophagy regulates HAVSMCs phenotypic changes in this progression. Thus we found MitoQ rescued VSMCs synthetic phenotype remodeling and mitophagy, which were further improved by PINK1 siRNA (Figs. 4, 6–8). Mitophagy is an important goalkeeper of mitochondrial quality control, which is mainly regulated by the PINK1/Parkin signal pathway [58]. When mitochondria are damaged, PINK1 cannot enter the mitochondria due to the decrease of the inner membrane potential, and it continuously accumulates on the outer mitochondrial membrane, recruiting Parkin in the cytoplasm, which is an E3 ubiquitin ligase, and then the activated Parkin ubiquitinates the outer mitochondrial membrane Protein 20 (Tom20), finally fused with lysosome and degraded [56]. Our results indicated MitoQ treatment restored appropriate mitophagy level in aorta or HAVSMCs by reducing mitochondrial oxidative stress, thus improving mitochondrial dysfunction and reducing tissue or cell damage. Mizumura et al. suggested cigarette smoke (CS) exposure caused mitochondrial ROS in lung epithelial cell to regulate PINK1 expression, and the structure and function of mitochondria in PINK1<sup>-/-</sup> mice were relatively complete after exposure to CS [59]. Mitochondrial defects and atherosclerotic lesions were reduced in PINK1<sup>-/-</sup> mice after apelin-13

treatment [60]. In general, PM<sub>2.5</sub> increased mitochondrial ROS overproduction in HAVSMCs, activated PINK1/Parkin-mediated mitophagy which causing mitochondrial dysfunction, while MitoQ treatment restored this pathogenetic process.

## 5. Conclusions

In summary, our data demonstrated that PM<sub>2.5</sub> exposure increased mitochondrial oxidative stress and activated mitophagy, accompanied by mitochondrial dynamics disorder and mitochondrial dysfunction, caused VSMCs synthetic phenotype remodeling and ultimately led to aortic fibrosis; while MitoQ treatment restored this pathogenetic process via mitochondrial ROS/PINK1/Parkin-mediated mitophagy. Our results suggest a new treatment strategy to alleviate vascular damage caused by short-term PM<sub>2.5</sub> exposure.

## Declaration of competing interest

The authors declare they have no conflict of interest.

## Acknowledgements

This work was supported by National Key Research and Development Program of China (2017YFC0211600, 2017YFC0211602, 2017YFC0211606), National Natural Science Foundation of China (91943301, 92043301), Beijing Natural Science Foundation Program and Scientific Research Key Program of Beijing Municipal Commission of Education (KZ202110025040) and Beijing Outstanding talent Training Program (2018000026833ZK56).

## References

- [1] M. Brauer, B. Casadei, R.A. Harrington, R. Kovacs, K. Sliwa, Taking a stand against air pollution - the impact on cardiovascular disease, *Eur. Heart J.* 143 (2021) e800–e804.
- [2] P. Joseph, D. Leong, M. McKee, S.S. Anand, J.-D. Schwalm, K. Teo, A. Mente, S. Yusuf, Reducing the global burden of cardiovascular disease, Part 1: the epidemiology and risk factors, *Circ. Res.* 121 (2017) 677–694.
- [3] P. Yin, M. Brauer, A.J. Cohen, H. Wang, J. Li, R.T. Burnett, J.D. Stanaway, K. Causey, S. Larson, W. Godwin, J. Frostad, A. Marks, L. Wang, M. Zhou, C.J. L. Murray, The effect of air pollution on deaths, disease burden, and life expectancy across China and its provinces, 1990–2017: an analysis for the Global Burden of Disease Study 2017, *Lancet Planet Health* 4 (2020) e386–e398.
- [4] S.G. Al-Kindi, R.D. Brook, S. Biswal, S. Rajagopalan, Environmental determinants of cardiovascular disease: lessons learned from air pollution, *Nat. Rev. Cardiol.* 17 (2020) 656–672.
- [5] R. Chen, A. Zhao, H. Chen, Z. Zhao, J. Cai, C. Wang, C. Yang, H. Li, X. Xu, S. Ha, T. Li, H. Kan, Cardiopulmonary benefits of reducing indoor particles of outdoor origin: a randomized, double-blind crossover trial of air purifiers, *J. Am. Coll. Cardiol.* 65 (2015) 2279–2287.
- [6] Y. Zheng, J. Fan, H.-W. Chen, E.-Q. Liu, *Trametes orientalis* polysaccharide alleviates PM-induced lung injury in mice through its antioxidant and anti-inflammatory activities, *Food Funct* 10 (2019) 8005–8015.
- [7] F. Ren, Y. Huang, Y. Tao, C. Ji, S. Aniaqu, Y. Jiang, T. Chen, Resveratrol protects against PM<sub>2.5</sub>-induced heart defects in zebrafish embryos as an antioxidant rather than as an AHR antagonist, *Toxicol. Appl. Pharmacol.* 398 (2020) 115029.
- [8] C. Huang, A.E. Moran, P.G. Coxson, X. Yang, F. Liu, J. Cao, K. Chen, M. Wang, J. He, L. Goldman, D. Zhao, P.L. Kinney, D. Gu, Potential cardiovascular and total mortality benefits of air pollution control in urban China, *Circulation* 136 (2017) 1575–1584.
- [9] T.-H. Lan, X.-Q. Huang, H.-M. Tan, Vascular fibrosis in atherosclerosis, *Cardiovasc. Pathol.* 22 (2013) 401–407.
- [10] S. Huang, S. You, J. Qian, C. Dai, S. Shen, J. Wang, W. Huang, G. Liang, G. Wu, Myeloid differentiation 2 deficiency attenuates AngII-induced arterial vascular oxidative stress, inflammation, and remodeling, *Aging (N Y)* 13 (2021) 4409–4427.
- [11] N. Shi, X. Mei, S.-Y. Chen, Smooth muscle cells in vascular remodeling, *Arterioscler. Thromb. Vasc. Biol.* 39 (2019) e247–e252.
- [12] L. Grevendonk, B.G. Janssen, C. Vanpoucke, W. Lefebvre, M. Hoxha, V. Bollati, T. S. Nawrot, Mitochondrial oxidative DNA damage and exposure to particulate air pollution in mother-newborn pairs, *Environ. Health* 15 (2016) 10.
- [13] Z. Guo, Z. Hong, W. Dong, C. Deng, R. Zhao, J. Xu, G. Zhuang, R. Zhang, PM-induced oxidative stress and mitochondrial damage in the nasal mucosa of rats, *Int. J. Environ. Res. Publ. Health* 14 (2017) 134.
- [14] S.I. Dikalov, A.E. Dikalova, Crosstalk between mitochondrial hyperacetylation and oxidative stress in vascular dysfunction and hypertension, *Antioxidants Redox Signal.* 31 (2019) 710–721.

- [15] P.H.G.M. Willems, R. Rossignol, C.E.J. Dieteren, M.P. Murphy, W.J.H. Koopman, Redox homeostasis and mitochondrial dynamics, *Cell Metabol.* 22 (2015) 207–218.
- [16] X. Liu, X. Zhao, X. Li, S. Lv, R. Ma, Y. Qi, A. Abulikemu, H. Duan, C. Guo, Y. Li, Z. Sun, PM triggered apoptosis in lung epithelial cells through the mitochondrial apoptotic way mediated by a ROS-DRP1-mitochondrial fission axis, *J. Hazard Mater.* 397 (2020) 122608.
- [17] J.-Y. Jin, X.-X. Wei, X.-L. Zhi, X.-H. Wang, D. Meng, Drp1-dependent mitochondrial fission in cardiovascular disease, *Acta Pharmacol. Sin.* 42 (2021) 655–664.
- [18] L. Tian, F. Potus, D. Wu, A. Dasgupta, K.-H. Chen, J. Mewburn, P. Lima, S. L. Archer, Increased drp1-mediated mitochondrial fission promotes proliferation and collagen production by right ventricular fibroblasts in experimental pulmonary arterial hypertension, *Front. Physiol.* 9 (2018) 828.
- [19] X. Zhuang, A. Maimaitijiang, Y. Li, H. Shi, X. Jiang, Salidroside inhibits high-glucose induced proliferation of vascular smooth muscle cells via inhibiting mitochondrial fission and oxidative stress, *Exp Ther Med* 14 (2017) 515–524.
- [20] C. Vázquez-Trincado, I. García-Carvajal, C. Pennanen, V. Parra, J.A. Hill, B. A. Rothermel, S. Lavandero, Mitochondrial dynamics, mitophagy and cardiovascular disease, *J. Physiol.* 594 (2016) 509–525.
- [21] M. Xu, X. Wang, L. Xu, H. Zhang, C. Li, Q. Liu, Y. Chen, K.F. Chung, I.M. Adcock, F. Li, Chronic lung inflammation and pulmonary fibrosis after multiple intranasal instillation of PM in mice, *Environ. Toxicol.* 36 (2021) 1434–1446.
- [22] S. Kostin, L. Pool, A. Elsässer, S. Hein, H.C.A. Drexler, E. Arnon, Y. Hayakawa, R. Zimmermann, E. Bauer, W.-P. Klövekorn, J. Schaper, Myocytes die by multiple mechanisms in failing human hearts, *Circ. Res.* 92 (2003) 715–724.
- [23] D.J. Cao, Z.V. Wang, P.K. Battiprolu, N. Jiang, C.R. Morales, Y. Kong, B. A. Rothermel, T.G. Gillette, J.A. Hill, Histone deacetylase (HDAC) inhibitors attenuate cardiac hypertrophy by suppressing autophagy, *Proc. Natl. Acad. Sci. U. S. A.* 108 (2011) 4123–4128.
- [24] H. Jin, A. Kanthasamy, A. Ghosh, V. Anantharam, B. Kalyanaraman, A. G. Kanthasamy, Mitochondria-targeted antioxidants for treatment of Parkinson's disease: preclinical and clinical outcomes, *Biochim. Biophys. Acta* 1842 (2014) 1282–1294.
- [25] R.A.J. Smith, M.P. Murphy, Animal and human studies with the mitochondria-targeted antioxidant MitoQ, *Ann. N. Y. Acad. Sci.* 1201 (2010).
- [26] K.Y. Goh, L. He, J. Song, M. Jinno, A.J. Rogers, P. Sethu, G.V. Halade, N. S. Rajasekaran, X. Liu, S.D. Prabhu, V. Darley-Usmar, A.R. Wende, L. Zhou, Mitochondria ameliorates pressure overload-induced cardiac fibrosis and left ventricular dysfunction in mice, *Redox Biol* 21 (2019) 101100.
- [27] Q. Lin, S. Li, N. Jiang, X. Shao, M. Zhang, H. Jin, Z. Zhang, J. Shen, Y. Zhou, W. Zhou, L. Gu, R. Lu, Z. Ni, PINK1-parkin pathway of mitophagy protects against contrast-induced acute kidney injury via decreasing mitochondrial ROS and NLRP3 inflammasome activation, *Redox Biol* 26 (2019) 101254.
- [28] C.H. Wiegman, C. Michaeloudes, G. Haji, P. Narang, C.J. Clarke, K.E. Russell, W. Bao, S. Pavlidis, P.J. Barnes, J. Kanerva, A. Bittner, N. Rao, M.P. Murphy, P. A. Kirkham, K.F. Chung, I.M. Adcock, Copdmap, Oxidative stress-induced mitochondrial dysfunction drives inflammation and airway smooth muscle remodeling in patients with chronic obstructive pulmonary disease, *J. Allergy Clin. Immunol.* 136 (2015) 769–780.
- [29] M.J. Rossman, J.R. Santos-Parker, C.A.C. Steward, N.Z. Bispham, L.M. Cuevas, H. L. Rosenberg, K.A. Woodward, M. Chonchol, R.A. Gioscia-Ryan, M.P. Murphy, D. R. Seals, Chronic supplementation with a mitochondrial antioxidant (MitoQ) improves vascular function in healthy older adults, *Hypertension* 71 (2018) 1056–1063.
- [30] R.A. Gioscia-Ryan, M.L. Battson, L.M. Cuevas, J.S. Eng, M.P. Murphy, D.R. Seals, Mitochondria-targeted antioxidant therapy with MitoQ ameliorates aortic stiffening in old mice, *J. Appl. Physiol.* 124 (2018) 1194–1202.
- [31] L. Kang, S. Liu, J. Li, Y. Tian, Y. Xue, X. Liu, The mitochondria-targeted antioxidant MitoQ protects against intervertebral disc degeneration by ameliorating mitochondrial dysfunction and redox imbalance, *Cell Prolif* 53 (2020), e12779.
- [32] R. Ning, Y. Shi, J. Jiang, S. Liang, Q. Xu, J. Duan, Z. Sun, Mitochondrial dysfunction drives persistent vascular fibrosis in rats after short-term exposure of PM<sub>2.5</sub>, *Sci. Total Environ.* 733 (2020) 139135.
- [33] R.D. Brook, J.R. Brook, B. Urch, R. Vincent, S. Rajagopalan, F. Silverman, Inhalation of fine particulate air pollution and ozone causes acute arterial vasoconstriction in healthy adults, *Circulation* 105 (2002) 1534–1536.
- [34] Y. Zhang, H. Hu, Y. Shi, X. Yang, L. Cao, J. Wu, C.O. Asweto, L. Feng, J. Duan, Z. Sun, <sup>1</sup>H-NMR-based metabolomics study on repeat dose toxicity of fine particulate matter in rats after intratracheal instillation, *Sci. Total Environ.* 589 (2017) 212–221.
- [35] J. Gao, J. Yuan, Q.e. Wang, T. Lei, X. Shen, B. Cui, F. Zhang, W. Ding, Z. Lu, Metformin protects against PM-induced lung injury and cardiac dysfunction independent of AMP-activated protein kinase  $\alpha 2$ , *Redox Biol* 28 (2020) 101345.
- [36] H. Tong, Dietary and pharmacological intervention to mitigate the cardiopulmonary effects of air pollution toxicity, *Biochim. Biophys. Acta* 1860 (2016) 2891–2898.
- [37] A. Milan, G. Zocaro, D. Leone, F. Tosello, I. Buraioli, D. Schiavone, F. Veglio, Current assessment of pulse wave velocity: comprehensive review of validation studies, *J. Hypertens.* 37 (2019) 1547–1557.
- [38] S.-Y. Chuang, C.-H. Bai, H.-M. Cheng, J.-R. Chen, W.-T. Yeh, P.-F. Hsu, W.-L. Liu, W.-H. Pan, Common carotid artery end-diastolic velocity is independently associated with future cardiovascular events, *Eur J Prev Cardiol* 23 (2016) 116–124.
- [39] R.O. Bude, J.M. Rubin, Relationship between the resistive index and vascular compliance and resistance, *Radiology* 211 (1999) 411–417.
- [40] W.W. Nichols, Clinical measurement of arterial stiffness obtained from noninvasive pressure waveforms, *Am. J. Hypertens.* 18 (2005).
- [41] M.E. Safar, Arterial stiffness as a risk factor for clinical hypertension, *Nat. Rev. Cardiol.* 15 (2018) 97–105.
- [42] C.-F. Wu, F.-H. Shen, Y.-R. Li, T.-M. Tsao, M.-J. Tsai, C.-C. Chen, J.-S. Hwang, S.H.-J. Hsu, H. Chao, K.-J. Chuang, C.C.K. Chou, Y.-N. Wang, C.-C. Ho, T.-C. Su, Association of short-term exposure to fine particulate matter and nitrogen dioxide with acute cardiovascular effects, *Sci. Total Environ.* 569–570 (2016) 300–305.
- [43] G.A. Wellenius, L.D. Boyle, E.H. Wilker, F.A. Sorond, B.A. Coull, P. Koutrakis, M. A. Mittleman, L.A. Lipsitz, Ambient fine particulate matter alters cerebral hemodynamics in the elderly, *Stroke* 44 (2013) 1532–1536.
- [44] A. Harvey, A.C. Montezano, R.A. Lopes, F. Rios, R.M. Touyz, Vascular fibrosis in aging and hypertension: molecular mechanisms and clinical implications, *Can. J. Cardiol.* 32 (2016) 659–668.
- [45] A. Frisanti, M. Philippova, P. Erne, T.J. Resink, Smooth muscle cell-driven vascular diseases and molecular mechanisms of VSMC plasticity, *Cell. Signal.* 52 (2018) 48–64.
- [46] A. Veerappan, A. Oskuei, G. Crowley, M. Mikhail, D. Ostrofsky, Z. Gironda, S. Vaidyanathan, Y.Z. Wadghiri, M. Liu, S. Kwon, A. Nolan, World trade center-cardiorespiratory and vascular dysfunction: assessing the phenotype and metabolome of a murine particulate matter exposure model, *Sci. Rep.* 10 (2020) 3130.
- [47] J. Jiang, S. Liang, J. Zhang, Z. Du, Q. Xu, J. Duan, Z. Sun, Melatonin ameliorates PM<sub>2.5</sub>-induced cardiac perivascular fibrosis through regulating mitochondrial redox homeostasis, *J. Pineal Res.* 70 (2021), e12686.
- [48] X. Miao, W. Li, B. Niu, J. Li, J. Sun, M. Qin, Z. Zhou, Mitochondrial dysfunction in endothelial cells induced by airborne fine particulate matter (<2.5  $\mu\text{m}$ ), *J. Appl. Toxicol.* 39 (2019) 1424–1432.
- [49] S.M. Yeligar, B.-Y. Kang, K.M. Bijli, J.M. Kleinhenz, T.C. Murphy, G. Torres, A. San Martin, R.L. Sutliff, C.M. Hart, PPAR $\gamma$  regulates mitochondrial structure and function and human pulmonary artery smooth muscle cell proliferation, *Am. J. Respir. Cell Mol. Biol.* 58 (2018) 648–657.
- [50] A.P. Davel, M. Lemos, L.M. Pastro, S.C. Pedro, P.A. de André, C. Hebeda, S. H. Farsky, P.H. Saldiva, L.V. Rossoni, Endothelial dysfunction in the pulmonary artery induced by concentrated fine particulate matter exposure is associated with local but not systemic inflammation, *Toxicology* 295 (2012) 39–46.
- [51] S. Muliylil, M. Narasimha, Mitochondrial ROS regulates cytoskeletal and mitochondrial remodeling to tune cell and tissue dynamics in a model for wound healing, *Dev. Cell* 28 (2014) 239–252.
- [52] G. Marsboom, P.T. Toth, J.J. Ryan, Z. Hong, X. Wu, Y.-H. Fang, T. Thenappan, L. Piao, H.J. Zhang, J. Pogoriler, Y. Chen, E. Morrow, E.K. Weir, J. Rehman, S. L. Archer, Dynamin-related protein 1-mediated mitochondrial mitotic fission permits hyperproliferation of vascular smooth muscle cells and offers a novel therapeutic target in pulmonary hypertension, *Circ. Res.* 110 (2012) 1484–1497.
- [53] A.O. Oyewole, M.A. Birch-Machin, Mitochondria-targeted antioxidants, *Faseb. J.* 29 (2015) 4766–4771.
- [54] D. Graham, N.N. Huynh, C.A. Hamilton, E. Beattie, R.A.J. Smith, H.M. Cochemé, M.P. Murphy, A.F. Dominiczak, Mitochondria-targeted antioxidant MitoQ10 improves endothelial function and attenuates cardiac hypertrophy, *Hypertension* 54 (2009) 322–328.
- [55] D. Yang, D. Xu, T. Wang, Z. Yuan, L. Liu, Y. Shen, F. Wen, Mitochondria-targeted antioxidant MitoQ ameliorates cigarette smoke-induced airway inflammation and mucus hypersecretion in mice, *Int. Immunopharmacol.* 90 (2021) 107149.
- [56] J.M. Bravo-San Pedro, G. Kroemer, L. Galluzzi, Autophagy and mitophagy in cardiovascular disease, *Circ. Res.* 120 (2017) 1812–1824.
- [57] K. Sachdeva, D.C. Do, Y. Zhang, X. Hu, J. Chen, P. Gao, Environmental exposures and asthma development: autophagy, mitophagy, and cellular senescence, *Front. Immunol.* 10 (2019) 2787.
- [58] G. Ashrafi, T.L. Schwarz, The pathways of mitophagy for quality control and clearance of mitochondria, *Cell Death Differ.* 20 (2013) 31–42.
- [59] K. Mizumura, S.M. Cloonan, K. Nakahira, A.R. Bhashyam, M. Cervo, T. Kitada, K. Glass, C.A. Owen, A. Mahmood, G.R. Washko, S. Hashimoto, S.W. Ryter, A.M. K. Choi, Mitophagy-dependent necroptosis contributes to the pathogenesis of COPD, *J. Clin. Invest.* 124 (2014) 3987–4003.
- [60] L. He, Q. Zhou, Z. Huang, J. Xu, H. Zhou, D. Lv, L. Lu, S. Huang, M. Tang, J. Zhong, J.-X. Chen, X. Luo, L. Li, L. Chen, PINK1/Parkin-mediated mitophagy promotes apelin-13-induced vascular smooth muscle cell proliferation by AMPK $\alpha$  and exacerbates atherosclerotic lesions, *J. Cell. Physiol.* 234 (2019) 8668–8682.